

DOCUMENT CONTROL SHEET

	ORIGINATOR'S REF. NLR-TP-2004-318	SECURITY CLASS. Unclassified		
ORIGINATOR National Aerospace Laboratory NLR, Amsterdam, The Netherlands				
TITLE An experimental study of landing gear wake/flap interaction noise				
Presented at the 10 th AIAA/CEAS Aeroacoustics Conference in Manchester, UK on 10-12 May 2004				
PERMISSION				
AUTHORS S. Oerlemans and M. Pott-Pollenske* <small>* German Aerospace Center DLR</small>	DATE August 2004	<table border="1" style="width: 100%; border-collapse: collapse;"> <tr> <td style="width: 50%;">PP 16</td> <td style="width: 50%;">REF 12</td> </tr> </table>	PP 16	REF 12
PP 16	REF 12			
DESCRIPTORS microphone array, airframe noise, interaction noise				
ABSTRACT <p> An experimental study was performed into landing gear wake/ flap interaction noise. From wake measurements on various landing gear models, it was established that the characteristics of the turbulent wake do not strongly depend on model scale or details of the model geometry. On this basis a generic main landing gear model was designed and the turbulent wake characteristics were determined from hot-wire measurements. Subsequently, acoustic wind tunnel tests were carried out on a 1:13 scaled 2D wing section including the generic main landing gear. The purpose of these measurements was to quantify interaction noise and to determine the factors influencing this noise source. In addition, possible noise reduction concepts were explored. Several measurement techniques were applied to determine the acoustic and aerodynamic characteristics of the flow. An out-of-flow microphone array was used to localize and quantify different noise sources, whereas the directivity of the noise was measured with farfield microphones. The turbulent wake characteristics were determined using (un)steady pressure transducers on the flap surface. To assess the important parameters for interaction noise, a number of model configurations was tested, including closed/open cavity, with/without wheels and varying gear position. Interaction noise reduction devices included a porous flap leading edge and flexible brushes at the trailing edge of the main wing element. The test results clearly indicate the presence of interaction noise radiated from the flap leading edge. It turns out that the interaction noise is most pronounced at low frequencies, where it dominates the noise from the landing gear itself. The interaction noise shows no pronounced radiation directivity or dependence on angle of attack - except for a low frequency forward arc radiation. The noise levels are found to scale with U^6 versus Strouhal number. The gear rather than the cavity is found to be the most important contributor to the turbulent wake impinging on the flap. Placing the gear more upstream results in a reduction of interaction noise in the order of a few dB. Even larger reductions can be obtained with a porous flap leading edge. </p>				



NLR-TP-2004-318

An experimental study of landing gear wake/flap interaction noise

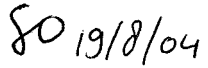


S. Oerlemans and M. Pott-Pollenske*

* German Aerospace Center DLR

This report is based on AIAA paper 2004-2886 presented at the 10th AIAA/CEAS Aeroacoustics Conference in Manchester, UK on 10-12 May 2004.

This report may be cited on condition that full credit is given to NLR and the authors.

Customer: National Aerospace Laboratory NLR
Working Plan number: AV.1.C.1
Owner: National Aerospace Laboratory NLR
Division: Aerospace Vehicles
Distribution: Unlimited
Classification title: Unclassified
August 2004

Approved by author:  19/8/04	Approved by project manager:  19/8/04.	Approved by project managing department:  23/8/04
--	---	---



Contents

I. Introduction	3
II. Gear Wake Characteristics	5
III. Interaction Noise Measurements	6
IV. Conclusions	16
Acknowledgements	16
References	16

27 Figures

(16 pages in total)



An Experimental Study of Landing Gear Wake/Flap Interaction Noise

Stefan Oerlemans*

National Aerospace Laboratory NLR, Emmeloord, The Netherlands

and

Michael Pott-Pollenske†

German Aerospace Center DLR, Braunschweig, Germany

An experimental study was performed into gear wake/ flap interaction noise. From wake measurements on various landing gear models, it was established that the characteristics of the turbulent wake do not strongly depend on model scale or details of the model geometry. On this basis a generic main landing gear model was designed and the turbulent wake characteristics were determined from hot-wire measurements. Subsequently, acoustic wind tunnel tests were carried out on a 1:13 scaled 2D wing section including the generic main landing gear. The purpose of these measurements was to quantify interaction noise and to determine the factors influencing this noise source. In addition, possible noise reduction concepts were explored. Several measurement techniques were applied to determine the acoustic and aerodynamic characteristics of the flow. An out-of-flow microphone array was used to localize and quantify different noise sources, whereas the directivity of the noise was measured with farfield microphones. The turbulent wake characteristics were determined using (un)steady pressure transducers on the flap surface. To assess the important parameters for interaction noise, a number of model configurations was tested, including closed/open cavity, with/without wheels and varying gear position. Interaction noise reduction devices included a porous flap leading edge and flexible brushes at the trailing edge of the main wing element. The test results clearly indicate the presence of interaction noise radiated from the flap leading edge. It turns out that the interaction noise is most pronounced at low frequencies, where it dominates the noise from the landing gear itself. The interaction noise shows no pronounced radiation directivity or dependence on angle of attack - except for a low frequency forward arc radiation. The noise levels are found to scale with U^6 versus Strouhal number. The gear rather than the cavity is found to be the most important contributor to the turbulent wake impinging on the flap. Placing the gear more upstream results in a reduction of interaction noise in the order of a few dB. Even larger reductions can be obtained with a porous flap leading edge.

I. Introduction

PREVIOUS research¹ indicated that noise due to landing gear and trailing edge flaps being deployed together can exceed the sum of the noise due to deployment of the individual devices. These observations suggest an interaction of the flap with the turbulent wake of the landing gear (Figure 1). However, up to now this mechanism has not been studied in detail. Therefore, in the framework of the European SILENCE(R) project, an experimental study was performed into gear wake/flap interaction noise. Acoustic wind tunnel tests were carried out on a 1:13 scaled 2D wing section including a generic main landing gear. The purpose of these measurements was to quantify interaction noise and to determine the factors influencing this noise source. In addition, possible noise reduction concepts were explored.

* Research engineer, Aeroacoustics Department, P.O. Box 153, 8300 AD Emmeloord, The Netherlands.

† Research engineer, Institute of Aerodynamics and Flow Technology, Lilienthalplatz 7, 38108 Braunschweig, Germany.



In view of the relatively small model scale, the effect of model scale on gear wake properties was investigated prior to the interaction noise measurements. Wake measurements were conducted downstream of (1) a 1:3 scaled center landing gear (CLG) in Airbus UK's Filton LSWT (closed test section) and (2) a 1:10 scaled CLG in DLR's Aeroacoustic Wind Tunnel Braunschweig (AWB, open jet). All main features of an Airbus A340 CLG were represented, e.g. main fitting, wheels, tires, drag stay, torque links and doors. The model fidelity was determined by the smaller model. For both measurements laminar vortex shedding was avoided by applying zig-zag tape on the cylindrical components of the gear positioned at 45° relative to the free stream flow direction. By using a rake of four cross hot-wire sensors, mean velocities, turbulence intensities and turbulence spectra were determined in three scan planes located downstream of the CLG, at axial distances of 3, 4 and 5 wheel diameters. Unsteady wake characteristics were acquired for frequencies up to 20 kHz and for free stream velocities of 20, 40 and 60 m/s.

Comparing the mean wake flow properties it turned out that aside from small differences (that may be related to the different test sections) for two model scales similar wake patterns were obtained both for mean velocities and turbulence intensities. The decay of turbulence intensity with increasing downstream distance behind the CLG is also similar for both model scales. Turbulence spectra obtained at different downstream positions were normalized and compared with the Von Kármán spectrum of normalized isotropic flow turbulence. The comparison showed good agreement between measured spectra at different downstream positions behind the CLG and the Von Kármán spectrum. Therefore the gear wake flow turbulence can be considered isotropic even for the most upstream measurement plane. On the basis of these results it can be stated that wake measurements with small-scaled models provide representative wake properties both for mean velocities and also for unsteady flow characteristic like turbulence intensities, turbulence spectra and wake decay.

Based on this conclusion a detailed 1:10 scaled Airbus A340 main landing gear (MLG) was used to determine the properties of the turbulent wake which is generated by a MLG, and impinges on the deployed flap during the approach phase of an aircraft. The main landing gear model was designed as detailed as possible at 1:10 scale (Figure 2) including the A340 undercarriage bay cavity. As for the CLG unsteady wake, data were acquired by means of a rake of cross hot-wires, for frequencies up to 20 kHz and for free stream velocities of 20, 40 and 60 m/s. The measurement planes were located downstream of the MLG model at axial distances of 2, 3 and 4 wheel diameters and at 5 main leg diameters. The axial mean velocity distribution showed a pronounced deficit downstream of the main leg and leg-door area. This deficit was accompanied by strong lateral flow components. No effect of small model details on high frequency disturbances was determined on either the turbulence distribution or the turbulence spectra. The turbulence spectra as obtained for different positions downstream of the MLG collapsed well for model scale frequencies above 300 Hz, which are in fact the acoustically important frequencies. Comparisons with the Von Kármán spectrum again confirmed the conclusion that the turbulent wake flow generated by the MLG is isotropic. Therefore the use of a simplified model, as in the present study, is justified.

The present paper focuses on the interaction noise measurements that were carried out at scale 1:13. Section II describes the design and wake characteristics of a generic landing gear model. Section III discusses acoustic wind tunnel tests on the gear model in combination with a 2D wing section. Interaction noise characteristics are determined for various configurations using several measurement techniques, such as a microphone array, farfield microphones and (un)steady pressure transducers on the flap surface. The conclusions are summarized in Section IV.

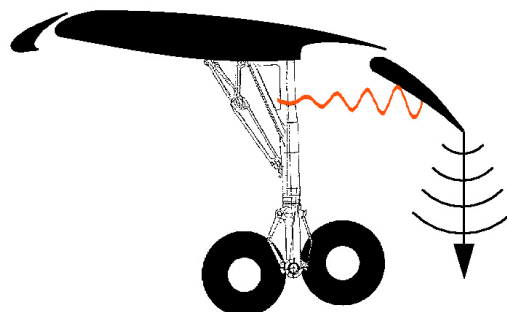


Figure 1: Schematic illustration of gear wake/flap interaction noise mechanism (not to scale).



Figure 2: Details of 1:10 scaled MLG.



II. Gear Wake Characteristics

This section describes the results of hot-wire measurements that were performed to characterize the turbulent wake of the generic landing gear. First the gear design will be discussed, followed by a description of the test set-up and the presentation of test results.

A. Landing Gear Model

For the 1:13 scaled landing gear model the main elements of an A340 main landing gear (MLG) were represented in a generic way. As explained above, the use of a simplified model at relatively small scale was justified by gear wake measurements at various model scales, which proved that the characteristics of the turbulent wake do not depend on model scale or on details of the model geometry. The main leg, drag stay, leg door, side-stay and down-lock linkage were represented, but smaller elements were omitted. The wheels were also omitted, since simple flow calculations indicated that their influence on the speed and turbulence levels at the position of the flap would be small. To check this assumption, during the interaction noise measurements one configuration was tested including wheels (see Section III). The main leg had a length of about 30 cm and a diameter of 27.5 mm. To prevent laminar vortex shedding, two 0.3 mm zig-zag transition strips were attached to the leg at 45° from the stagnation line. The cylindrical part of the side-stay was treated with trip wires of 1 mm diameter.

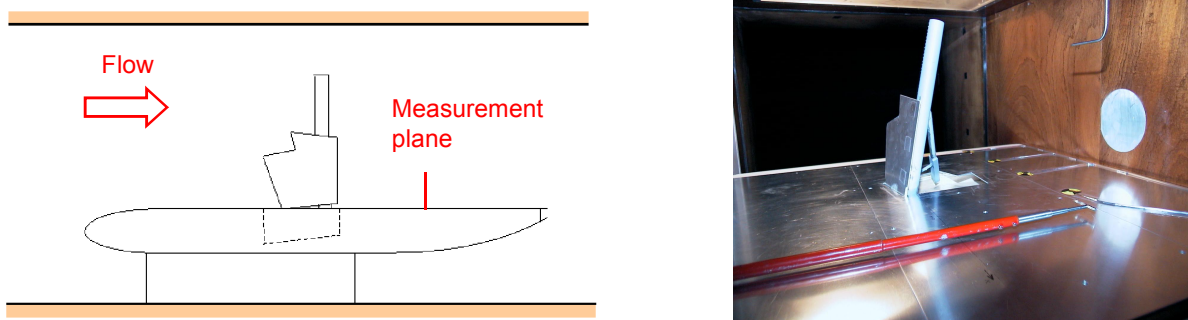


Figure 3: Test set-up for wake measurements on the generic landing gear in the DNW-PLST wind tunnel. The support sting for the hot-wire probe is shown in red (right).

B. Test Set-Up

The wake measurements were performed in the closed 0.8 x 0.6 m² test section of the DNW-PLST low speed wind tunnel, using hot-wires to determine velocity profiles and turbulence characteristics. The landing gear model was mounted on a ground board to obtain a realistic boundary layer at the location of the gear (Figure 3). The ground board also contained a scaled A340 cavity with variable depth. Most of the hot-wire measurements were performed at a distance of 217 mm downstream of the main leg (Figure 3). This position is beyond the location where the flap trailing edge would be located (i.e. at 150 mm), but the turbulence intensities more upstream were considered to too high for reliable hot-wire measurements. Hot-wire measurements were conducted on a rectangular grid in steps of 5 or 10 mm depending on flow field variations. The measurement grid was located close to the surface, because this is the part of the wake that impinges on the flap. Since for the generation of interaction noise both the axial and vertical turbulence intensities were considered most important, a cross wire was used in the vertical plane. For a number of configurations also lateral turbulence intensities were measured by rotating the cross wire by 90°. The unsteady hot-wire data were acquired at a sample frequency of 49 kHz and a measurement time of 10 s for each grid point. The turbulence intensities and spectra were normalized by the tunnel speed. The frequency resolution in the spectra is 39 Hz. Data were taken for two different cavity depths and for a closed cavity, with and without landing gear. The nominal wind speed was 40 m/s.

C. Results

For conciseness, wake results will only be presented for a standard landing configuration, i.e. an open cavity with landing gear, where the cavity depth corresponds to the interaction noise measurements discussed in Section III. Figure 4 shows the axial speed and turbulence distributions in the landing gear wake. It can be seen that the lowest velocity of $U/U_0=0.5$ occurs close to the supporting wall, while the cross flow field is dominated by a

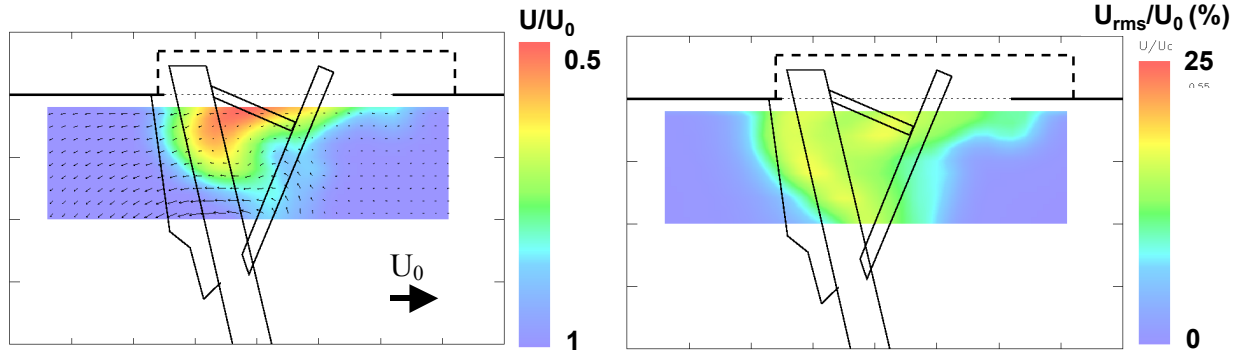


Figure 4: Axial velocity (left) and axial turbulence (right) distributions behind the generic landing gear with open cavity. The left plot also shows the corresponding cross-velocity vectors (the size of the reference arrow corresponds to the magnitude of U_0).

vortex which was found to originate from the leg door. Axial turbulence intensities of up to 18% are observed. The lateral turbulence showed similar intensities, while the vertical turbulence was slightly lower (up to 15%).

Comparison with 'gear only' and 'cavity only' configurations (not shown here) indicated that practically all wake turbulence originates from the gear rather than the cavity, although the cavity does influence the shape of the turbulence distribution. Besides the distribution of turbulence intensities, the spectral content of the turbulence is also important for the interaction noise mechanism. Figure 5 shows the axial turbulence spectra at several locations in the turbulent wake. Interestingly, this plot shows that at all locations in the turbulent wake the turbulence spectra coincide for frequencies higher than about 300 Hz (model scale). This is in good agreement with earlier wake measurements on a detailed 1:10 scaled MLG model (see Section I). Thus, local differences in turbulence intensity (as shown in Figure 4) stem from low-frequency turbulence, i.e. from frequencies below 300 Hz model scale. Assuming a frequency scaling factor of 13 (same as model scale), model scale frequencies below 300 Hz correspond to full-scale frequencies below 23 Hz, which are acoustically not important due to the A-weighting. Thus, for acoustically important frequencies the turbulence spectra at different positions in the wake coincide. For frequencies between about 300 Hz and 9 kHz level spectra decay according to a $-5/3$ slope, which corresponds to the Kolmogoroff spectrum law for isotropic turbulence in the inertial subrange. This spectrum is independent of the conditions of turbulence formation. The same observations were made for the wake measurements at larger scales (Section I), and confirm that the characteristics of the turbulent wake (for acoustically relevant frequencies) do not depend on details of the model geometry.

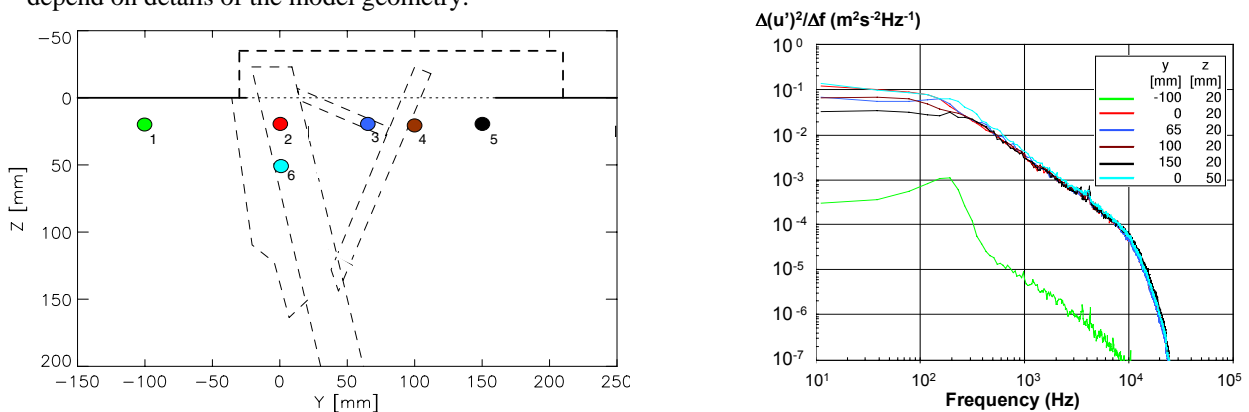


Figure 5 Axial turbulence spectra at several locations behind the generic landing gear with open cavity.

III. Interaction Noise Measurements

This section describes the acoustic wind tunnel measurements that were performed to characterize the interaction noise mechanism. First the test set-up will be described (Section III-A), followed by a description of the different



experimental techniques, i.e. acoustic array, farfield noise, and unsteady surface pressures (Sections III-B to III-D). In Section III-E the experimental results for the different configurations are presented.

A. Test Set-Up and Program

The tests were carried out in DLR's Aeroacoustic Wind Tunnel AWB (Figure 6). The AWB is an open jet wind tunnel with a rectangular nozzle of 1.2 m height and 0.8 m width. The test section downstream of the nozzle is surrounded by an anechoic room. Two vertical endplates are mounted to the sides of the nozzle, providing a semi-open test section for airframe noise measurements. To suppress reflections, the endplates are acoustically lined with a 0.03 m layer of sound absorbing foam. Due to the open jet set-up, the effective angle of attack is smaller than the geometrical angle of attack. The magnitude of this 'open jet effect' depends on the dimensions of the wind tunnel and the model chord. Based on measurements for this model dimension, the effect on angle of attack could be determined to $\Delta\alpha = -8^\circ$. This corresponds to calculations from Barlow, Rae and Pope². In the following discussion of test results, all data will be referenced to effective angles of attack.

The baseline model was a 2D three-element high-lift wing in landing configuration, consisting of slat, main wing and flap. The model (Figure 7) was placed 0.10 m above the wind tunnel axis and included a scaled A340 undercarriage bay cavity, in which the generic main landing gear (see Section II) was mounted. With respect to the landing gear scale the average cavity depth should have been 0.062 m. Due to the limited thickness of the main wing element, only 0.032 m average cavity depth could be realized. In contrast to the set-up as depicted in Figure 7, the landing gear generally had no wheels (except for a few data points), since these are not considered to be important for the turbulence impinging on the flap leading edge (see Section II-A).

Measurements were conducted for various configurations, including closed/open cavity, with/without wheels and varying gear positions relative to the flap. For the measurements with varying gear position, a generic gear was used, which simply consisted of a cylinder with the same dimensions and orientation as the main leg. Interaction noise reduction devices were also investigated, and included a porous flap leading edge and flexible brushes at the trailing edges of the main wing element. All configurations were tested for three wind speeds (20, 40, and 57 m/s) and three effective angles of attack (4° , 7° , and 11°).

B. Acoustic Array Measurements

The out-of-flow acoustic array consisted of 96 ½-inch LinearX M51 microphones mounted in an open metal grid, and was designed for maximum side-lobe suppression at frequencies between 1 and 25 kHz³. To obtain high resolution at low frequencies, the array dimensions need to be rather large (1.0 x 1.0 m²). The array was placed out of flow at a vertical distance of 1.0 m below the tunnel axis (1.1 m below the model). This relatively small distance between the array and the model was chosen to obtain maximum signal-to-noise ratio and high resolution at low frequencies. The center of the array was placed at the same lateral position as the tunnel axis, at a polar radiation angle of about 75° with respect to the upstream direction (same as farfield microphone M3, see Figure 10).

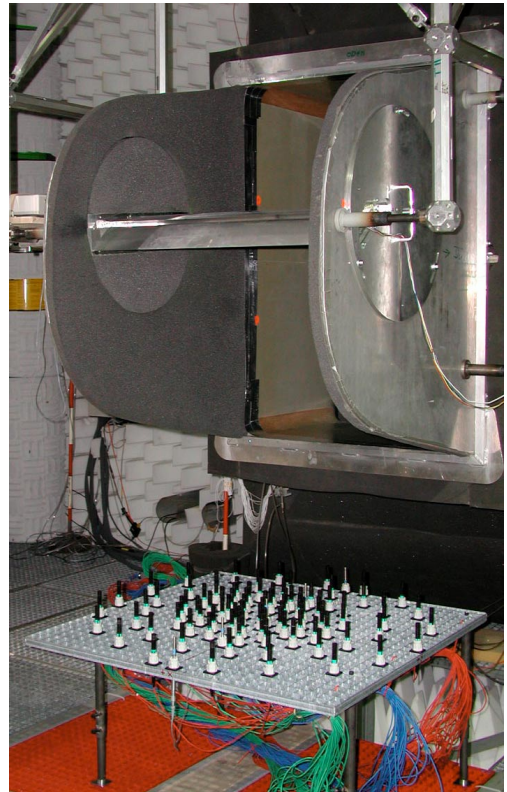


Figure 6 Test set-up in DLR's acoustic wind tunnel AWB. The microphone array is placed below the test section.

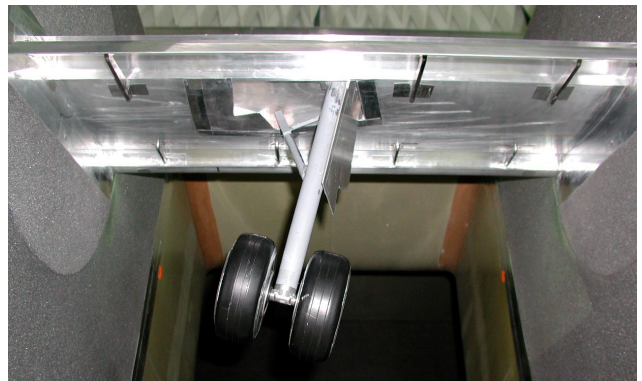


Figure 7: Close-up of 2D wing model with the generic landing gear, including wheels (looking upstream).



Acoustic data from the array microphones were synchronously measured at a sample frequency of 102.4 kHz and a measurement time of 30 s. A 500 Hz high-pass filter was used to enhance the dynamic range. The acoustic data were processed using a block size of 4096 with a Hanning window and an overlap of 50%, yielding 1500 averages and a narrowband frequency resolution of 25 Hz. The frequency response of the individual array microphones was taken from calibration sheets. Conventional beamforming⁴ was used to obtain acoustic source plots in 1/3-octave bands. To improve the resolution and suppress background noise from the tunnel, the main diagonal in the cross power matrix (autopowers) was discarded. In addition, a spatial window was applied to the microphone signals, which corrects for the variation in microphone density over the surface of the array, and which reduces the effective array aperture with increasing frequency. The purpose of this spatial shading was to improve the array resolution at low frequencies, and to reduce coherence loss effects at high frequencies. The effect of sound refraction by the tunnel shear layer was corrected using a simplified Amiet method⁵. The array scan plane was placed in the plane of the model and rotated in accordance with the angle of attack. The scan resolution was 1 cm in both directions and the scan levels were referenced towards a distance of 0.282 m $[(4\pi)^{-1/2}]$, so that for a monopole source the peak level in the source plot corresponds to the Sound Power Level.

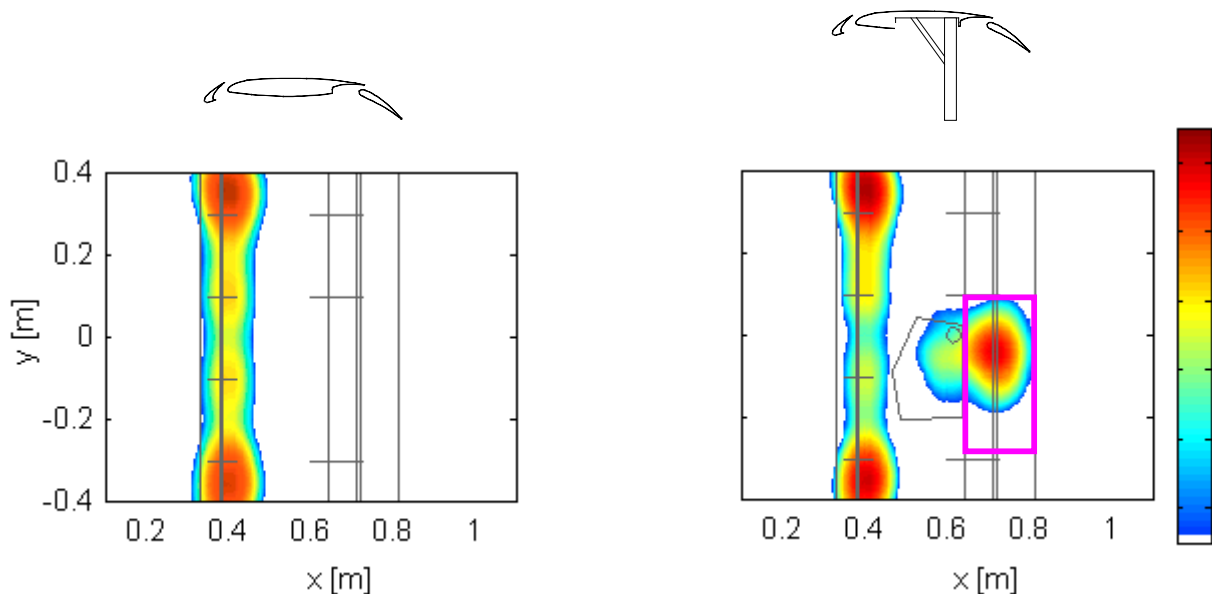


Figure 8: Acoustic source plots of 2D slat-wing-flap without (left) and with (right) landing gear installed, showing interaction noise from the flap leading edge (flow is from left to right) The model contours are indicated by the gray lines. The dynamic range of the color scale is 12 dB. The right plot shows the power integration contour (in pink) used for quantification of interaction noise.

Examples of acoustic source plots are presented in [Figure 8](#) for the baseline and standard landing configuration. The baseline configuration is the 2D slat-wing-flap, the standard configuration also has the gear (without wheels) and the cavity. Besides the noise sources at the slat, the right plot clearly shows a noise source at the position of the flap leading edge, downstream of the gear. Since this source is not present when the gear is absent, it must be caused by an interaction effect. Note that in principle this noise source could also be located at the trailing edge of the wing main element. However, in the discussion of the results it will be shown that it is most likely located at the flap leading edge.

[Figure 9](#) shows acoustic source plots at several frequencies for the standard landing configuration at 40 m/s. It turns out that at low frequencies the interaction noise dominates the noise from the generic gear itself, while at frequencies above 4 kHz the noise from the gear becomes more important. At 20 and 57 m/s this transition occurred around 2.5 and 5 kHz respectively.

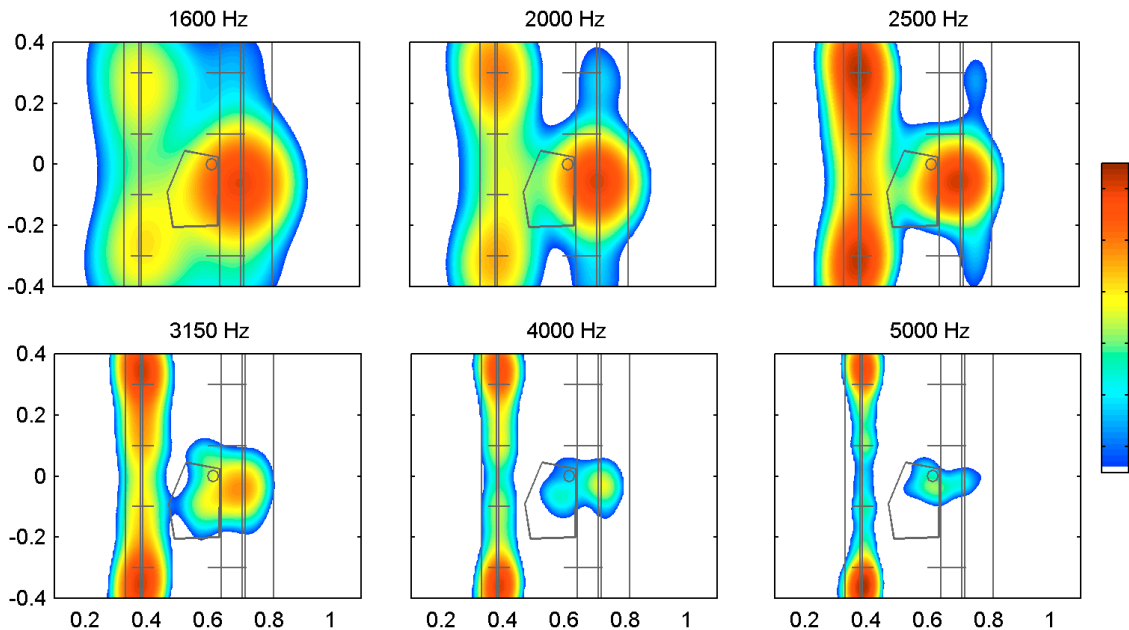


Figure 9: Acoustic source plots for standard landing configuration, illustrating gear wake/flap interaction noise at 40 m/s and $\alpha=7^\circ$. The flow goes from left to right. The dynamic range of the color scale is 12 dB.

To obtain quantified interaction noise levels, the acoustic source plots were further processed using a power integration method. The integration technique is similar to the simplified method in Ref.⁶, but it discards negative ‘source powers’ in the acoustic source plot⁷. The main diagonal of the cross power matrix was discarded to prevent tunnel background noise from obscuring the calculated airfoil noise levels^{7,8}. To separate interaction noise from other noise sources on the model (e.g. at the model-endplate junction), an integration contour was defined at the flap leading edge (Figure 8). By using an integration contour rather than peak levels, broadening of lobes in the source plots (due to coherence loss) is captured. Note that the integrated levels at higher frequencies may be partly caused by noise from the gear itself, which ‘leaks’ into the integration contour. The resulting integrated spectra provide the Sound Power Level of the interaction noise in 1/3-octave bands.

C. Farfield Noise Measurements

To collect directivity information in the farfield, five ¼-inch B&K 4136 pressure type microphones were mounted in the same grid as the array microphones. The microphones were aligned below the wind tunnel axis, providing directivity data for polar radiation angles (with respect to the flap leading edge) between 54° and 103° (Figure 10). The farfield noise signals were acquired with a 100 kHz sampling rate, and processed to a frequency resolution of 24.4 Hz. The signals were filtered through a 20 Hz high pass filter and analyzed up to 40 kHz in 1/3-octave bands, including corrections for background noise, microphone directivity, shear layer refraction, source convection, convective amplification and atmospheric absorption. Background noise correction was only performed for signal-to-noise ratios > 2 dB, otherwise measured data were deleted. Sound pressure levels were then referenced towards a constant radiation distance of 1 m. The calculation of ‘interaction noise’ spectra was performed by subtracting sound intensities as determined for the baseline configuration (i.e. the 2D wing without gear and cavity). It should be emphasized that the resulting level spectra include both interaction noise and noise from the landing gear itself. For level differences (relative to the baseline configuration) of less than 0.5 dB, data were deleted.

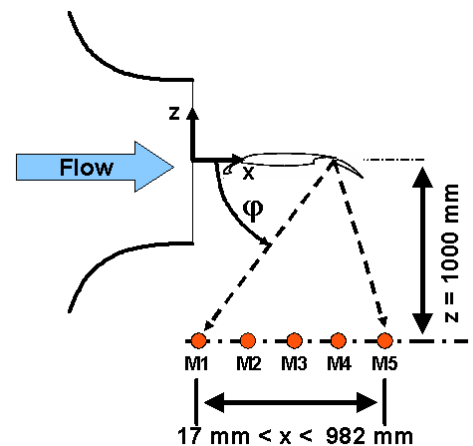


Figure 10: Farfield microphone set-up.



D. Unsteady Surface Pressure Measurements

The flap leading edge was instrumented with 36 Knowles EK-Series miniature electret condenser microphones, in order to characterize the turbulent wake impinging on the flap by means of unsteady surface pressures. The sensors were located downstream of the landing gear in six rows starting at a 5% chord position on the suction side and ranging to 68% chord on the pressure side. The chord- and spanwise positions of the unsteady surface pressure sensors are illustrated in Figure 11. Unsteady surface pressure signals were acquired up to 100 kHz and processed to a 24.4 Hz frequency resolution. According to the specifications of the miniature sensors, data were analyzed only up to 20 kHz in 1/3-octave bands, including a correction for the individual sensor’s frequency response relative to the calibrated linear response of a reference microphone.

Unsteady surface pressures can be understood as a footprint of the flow turbulence impinging on the surface and thus be used to identify noise source mechanisms^{9,10}. For the present study they were applied to characterize the turbulent wake generated by the landing gear impinging on the flap. As an example, Figure 12 shows measured spectra for sensor no. 4.6, which is located at 27% chord on the pressure side (red marked sensor in row 4, Figure 11). It can be seen that the surface pressure spectra are characterized by a low frequency level maximum, ranging from 200 to 1600 Hz, followed by a rapid level decrease of up to 20 dB for 10 kHz and above. It has to be stated that surface pressure spectra for $U_\infty = 20$ m/s showed spurious shapes. Therefore these data were deleted. Furthermore, for the highest wind speed of 57 m/s, sensor overload occurred for almost all configurations in row no. 1 (5% chord, suction side). Therefore, these data were deleted for the highest wind speed.

To check the validity of the measured data, the spectra for the baseline configuration were normalized with respect to the flow velocity. Local flow parameters, like boundary layer displacement thickness and local velocity, were not available at each sensor position. Therefore, the free stream velocity U_∞ was chosen to reference the pressure levels to free stream dynamic pressure, plotted versus Strouhal number based on an arbitrary length scale of 1 m. A U_∞^4 speed dependence was assumed.

$$20 * \log(P_s/q) = L_{meas} - 40 * \log(U_\infty/U_{ref}) - const.$$

$$Sr = f * 1 / U_\infty$$

Chordwise position of sensor rows

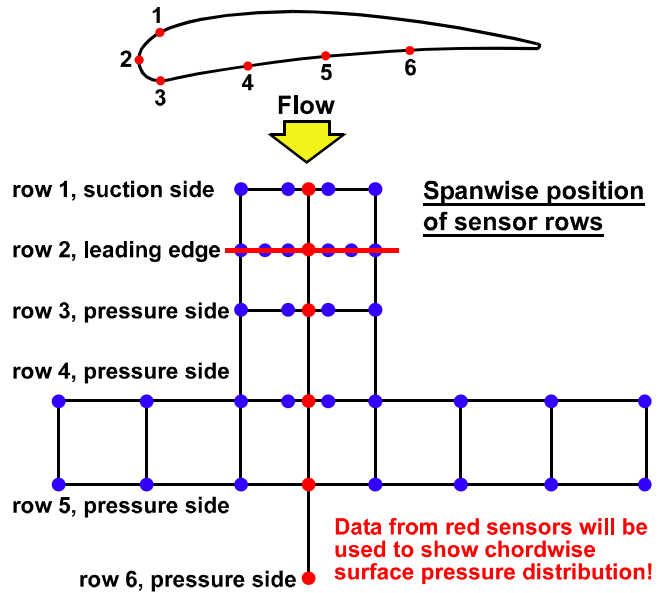


Figure 11: Positions of unsteady surface pressure sensors.

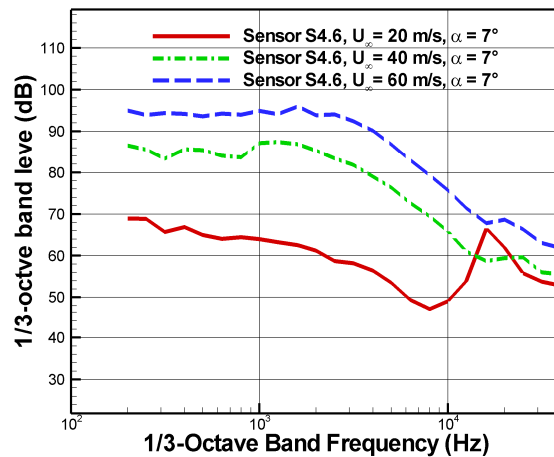


Figure 12: As measured surface pressure spectra at sensor no. 4.6, for the baseline configuration.

Pressure level normalization, $U_{ref} = 100$ m/s

Strouhal number definition

As depicted in Figure 13 the normalized spectra exhibit good agreement for free stream velocities $U_\infty = 40$ m/s and 57 m/s. These results prove that the measured flap surface pressure intensities scale according to a 4th power law versus Strouhal number, and therefore can be considered as a valid measure to describe the turbulent flow around



the flap. The same speed dependence was also found for the other configurations. Therefore, surface pressure results will be shown only for the intermediate wind speed $U_\infty = 40\text{ m/s}$ and a 7° effective angle of attack.

From the total amount of unsteady surface pressure data, results will be presented only for a limited number of configurations, in order to identify the effects of the different configurations on flap surface pressures. These results will be presented in terms of contour plots or chordwise surface pressure level distributions, depicted for the 1 kHz 1/3-octave band.

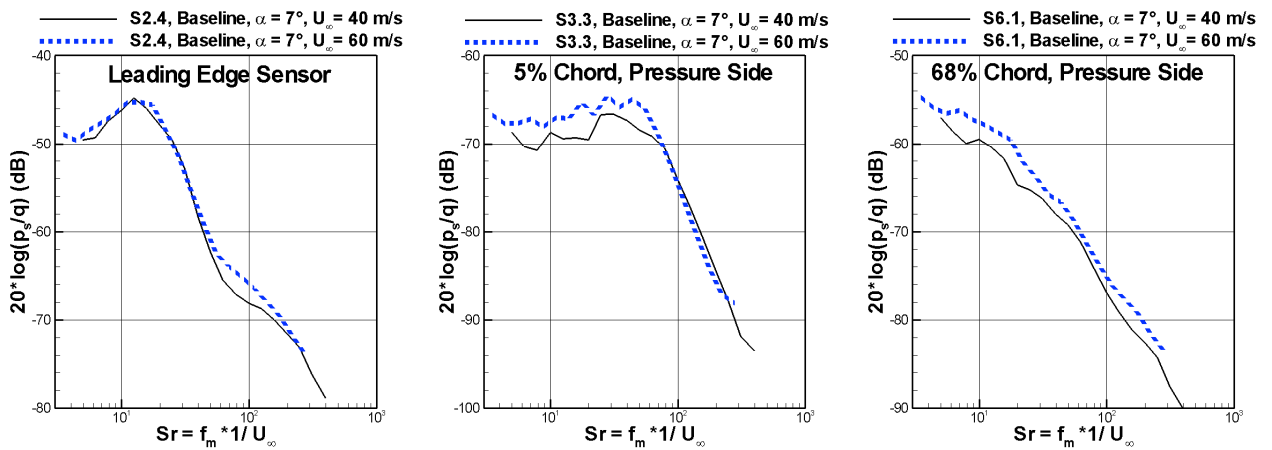


Figure 13: Normalized surface pressure spectra for the baseline configuration.

E. Discussion of Results

In this section the acoustic and aerodynamic results will be discussed for the different configurations that were tested: the standard landing configuration, the separate effect of gear and cavity, varying gear position, the effect of wheels, and finally the reduction devices.

1. Standard Landing Configuration

As explained in Section III-B, quantitative interaction noise spectra were determined using an integration contour around the flap leading edge downstream of the gear. This enables an assessment of the dependence of noise levels on speed and angle of attack. Interaction noise spectra for the three measured wind speeds are shown in Figure 14, both in physical and normalized quantities. As mentioned before, the levels at higher frequencies may be partly caused by noise from the gear itself. The normalized spectra are shown as a function of the Strouhal number, which is based on the mean flap thickness of 0.015 m. Normalized data are only shown for Strouhal numbers where

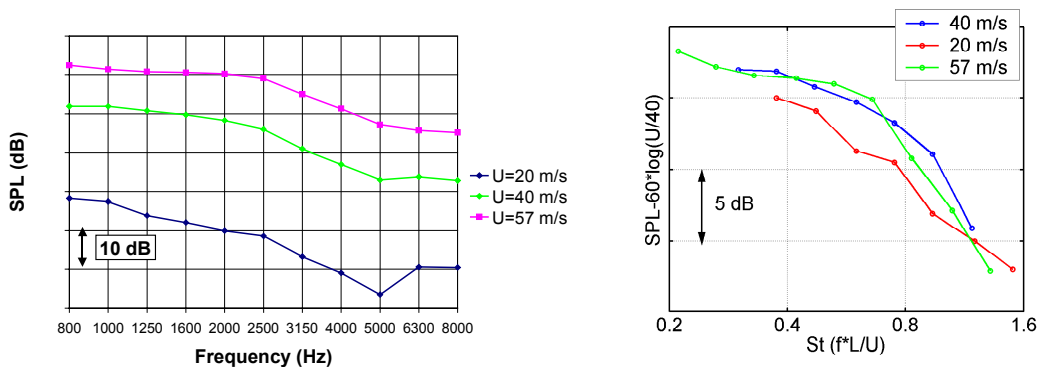


Figure 14: Speed dependence of interaction noise for standard landing configuration. The left plot shows the measured spectra, the right plot shows normalized spectra.



interaction noise was visible in the acoustic source plots. The normalized plot shows that a good data collapse is obtained when a 6th power law is used, although the 20 m/s line is slightly lower than the other two. The 6th power law is in good agreement with theoretical predictions of inflow turbulence noise¹¹ and with inflow turbulence noise measurements on isolated airfoils¹². Figure 15 shows that the effect of angle of attack on interaction noise is small. For low frequencies interaction noise seems to decrease slightly with increasing angle-of-attack. This may be due to a decrease in pressure side flow speed for increasing angle of attack, as observed from steady pressure transducers on the flap surface. The small differences around 5 kHz may be due to a change in the noise from the gear itself. Since the 6th power speed dependence and the small effect of angle of attack were found for all other configurations as well, in the remainder of this paper array results will only be presented for the intermediate wind speed ($U_\infty = 40$ m/s) and an effective angle of attack of 7°.

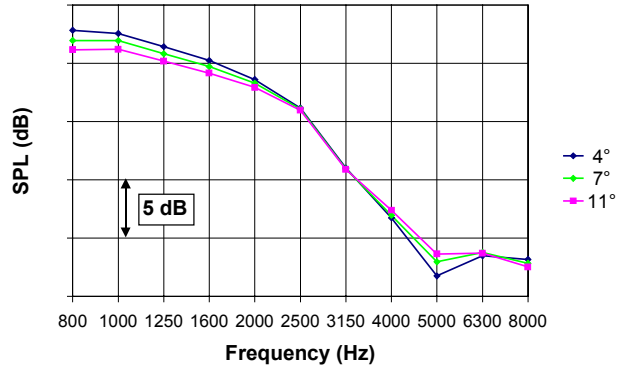


Figure 15: Angle of attack dependence of interaction noise for standard landing configuration ($U_\infty = 40$ m/s).

Since the 6th power speed dependence and the small effect of angle of attack were found for all other configurations as well, in the remainder of this paper array results will only be presented for the intermediate wind speed ($U_\infty = 40$ m/s) and an effective angle of attack of 7°.

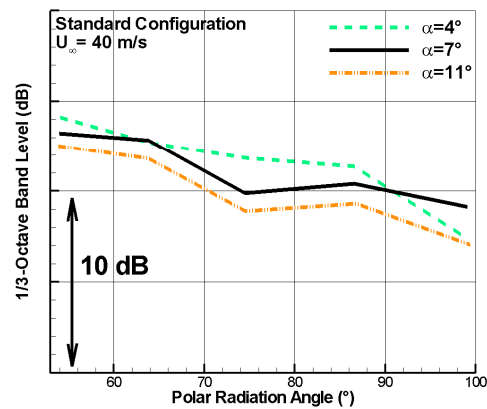
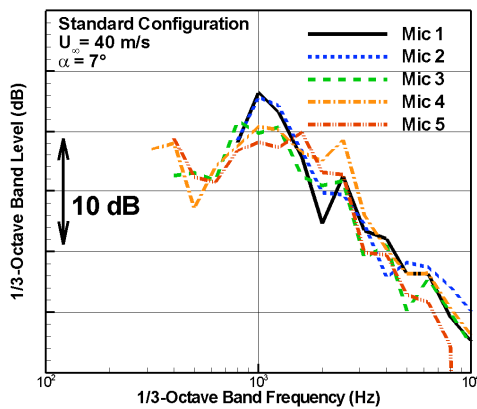


Figure 16: Standard configuration: farfield noise spectra (left) and directivity for $f_m = 1$ kHz (right).

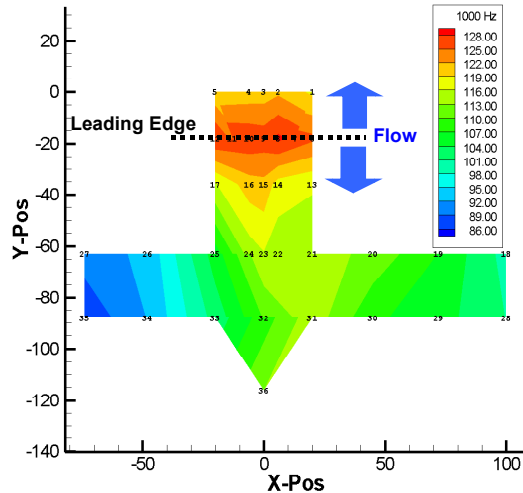
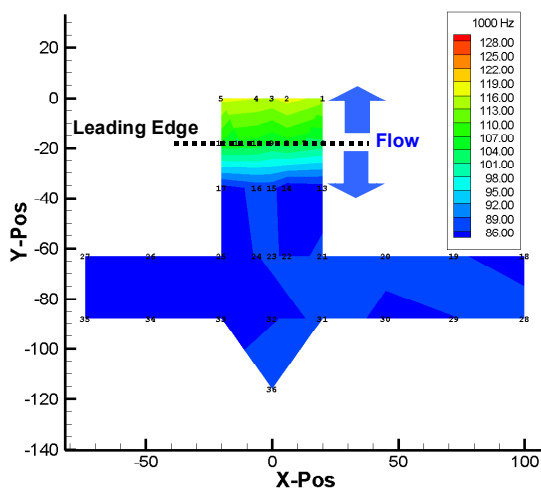


Figure 17: Comparison of baseline (left) and standard landing configuration for $f_m = 1000$ Hz, $U_\infty = 40$ m/s, $\alpha = 7^\circ$.



In addition to the results as described above, the farfield data enable the investigation of directivity effects. The spectra depicted in [Figure 16](#) show a level maximum at 1000 Hz for all microphone locations. The directivity plot for this frequency exhibits a slight forward arc directivity level maximum. For higher frequencies no pronounced directivity effect can be detected. Similar to [Figure 15](#), [Figure 16](#) (right) shows that, at 1 kHz and around a polar angle of 75° (where the array is located), interaction noise increases slightly with decreasing angle of attack.

Regarding the unsteady surface pressure results, a significant increase of pressure levels can be observed for every sensor row ([Figure 17](#)). At 1 kHz, which represents maximum unsteady pressure levels, high levels occur in particular at the flap leading edge. This observation is consistent with the array results, which showed prominent noise radiation from the flap leading edge ([Figure 8](#)), and supports the view that the interaction noise is radiated from the flap leading edge, rather than the trailing edge of the main wing element.

2. Separate Effect of Gear and Cavity

For the configuration with both the landing gear and the open undercarriage bay cavity it is not possible to determine whether the increased pressure levels are caused by the open cavity turbulent shear layer turbulence or by the landing gear wake flow. To assess the respective effects of the gear and/or the cavity on the interaction noise separately, the 'gear only' (cavity closed) and 'cavity only' (no gear) configurations were tested ([Figure 18](#)). As a lower limit, the baseline configuration (i.e. the 2D wing without gear and cavity) is shown as well. It can be seen that the 'gear only' configuration produces almost as much noise as the standard landing configuration (i.e. with gear and cavity), while the 'cavity only' configuration is significantly quieter. This illustrates that the gear, rather than the cavity, is the major contributor to the turbulent wake impinging on the flap leading edge. This finding is in good agreement with the wake measurements described in Section II. For frequencies of 5 kHz and higher the levels appear to be influenced by noise from the gear itself.

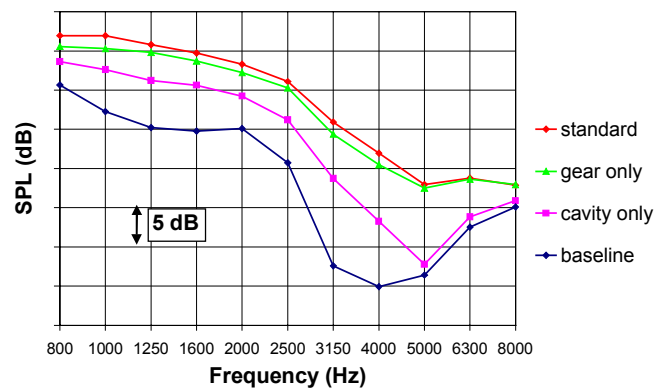


Figure 18: Separate effect of gear and cavity on interaction noise ($U_\infty = 40$ m/s, $\alpha = 7^\circ$).

The surface pressure results for the 'gear only' and 'cavity only' configurations are shown in [Figure 19](#). In addition, chordwise surface pressure distributions for the baseline, standard, 'gear only' and 'cavity only' configurations are shown in [Figure 20](#) for the $x = 0$ cut (for the definition of the ordinate y refer to [Figure 19](#)). It turns out that turbulence produced by the open cavity is convected close to the main wing pressure side surface

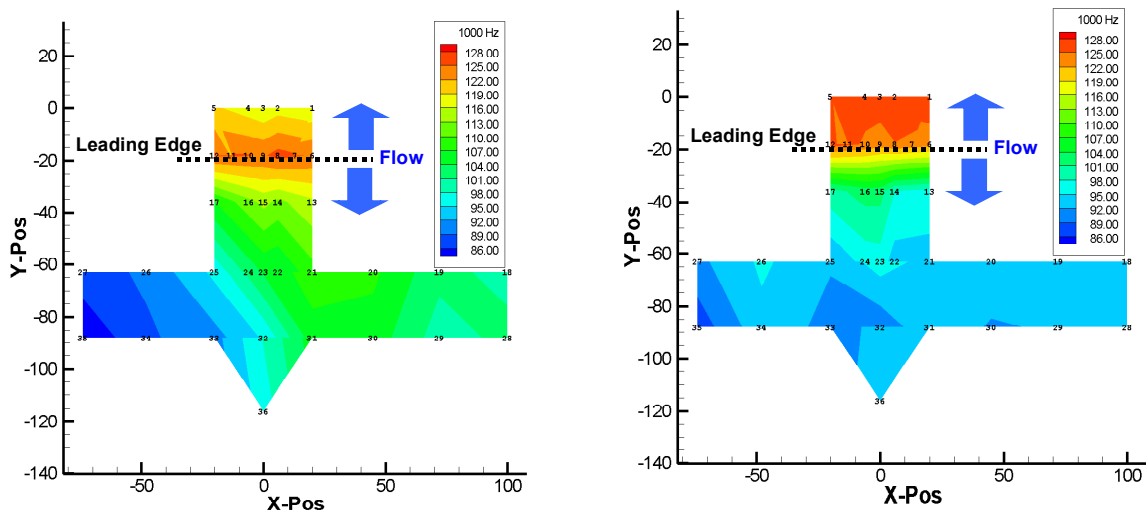


Figure 19: Comparison of gear only (left side) and cavity only (right) configuration for $f_m = 1000$ Hz, $U_\infty = 40$ m/s, $\alpha = 7^\circ$.



passing through the flap slot while the gear wake itself mainly hits the flap's pressure side (Figure 21). This is in good agreement with the acoustic results, where the gear was shown to be the major contributor to the interaction noise. Interestingly, the suction side pressures for 'cavity only' are higher than for the standard landing configuration. Apparently the presence of the gear reduces the amount of turbulence convected through the gap.

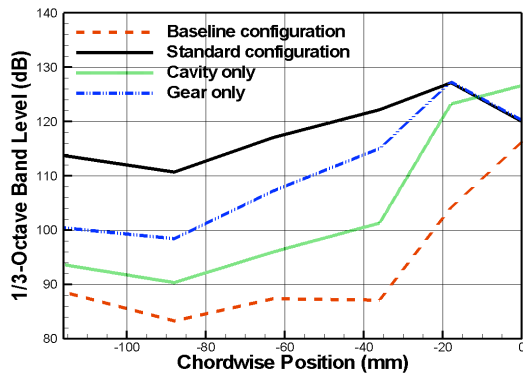


Figure 20: Chordwise surface pressure distribution for baseline, standard, gear only and cavity only configuration, $U_\infty = 40\text{m/s}$, $\alpha = 7^\circ$, $f_m=1000\text{ Hz}$.

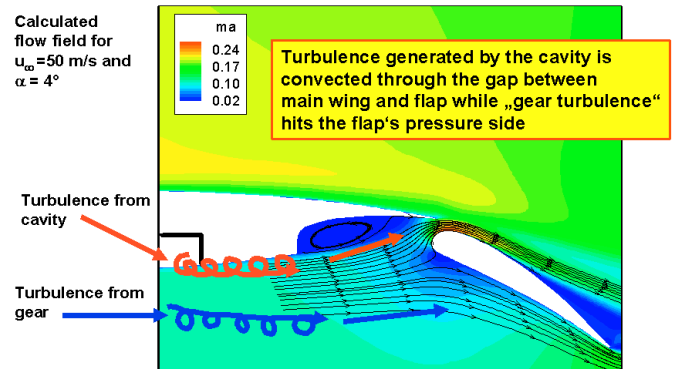


Figure 21: Convection of turbulence to flap.

3. Varying Gear Position

The influence of gear position on the interaction noise characteristics was investigated by replacing the gear by a cylinder with variable streamwise distance to the flap leading edge. Three cylinder positions were measured: one close to the downstream cavity edge (standard gear position), one close to the upstream cavity edge, and one intermediate position. Figure 22 shows that the interaction noise spectrum for the cylinder at the standard position is very similar to the standard spectrum (with gear and cavity), although the levels are slightly lower. Nevertheless the cylinder seems to be well suited for simulating the effect of gear position. The interaction noise spectra for the different cylinder positions (Figure 22) show that by moving the cylinder upstream, noise reductions of up to about 5 dB can be obtained at higher frequencies. Apparently the broadening of the wake is overcompensated by the decay in turbulence intensity. At low frequencies the differences are small. It should be noted that the high-frequency reduction may be partly due to a decreased contribution of gear noise, since the gear is further away from the integration contour (see also next paragraph).

As shown in Figure 23, the surface pressure distributions (at 1 kHz) for the cylinder in downstream, middle and upstream position exhibit level differences of 1 to 2 dB at the flap leading edge and up to 4 dB further downstream towards the flap trailing edge. Moving the cylinder to a more upstream position leads to a small decrease in surface pressure levels. The surface pressure distribution at 5 kHz was similar to 1 kHz, indicating that at least part of the high-frequency reduction observed in the array spectra is due to a reduction of interaction noise.

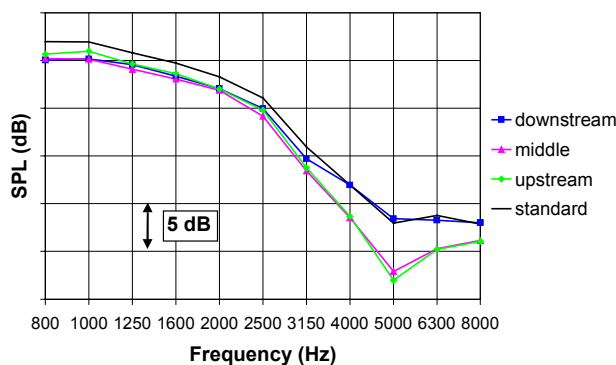


Figure 22: Effect of gear position on interaction noise ($U_\infty = 40\text{ m/s}$, $\alpha=7^\circ$).

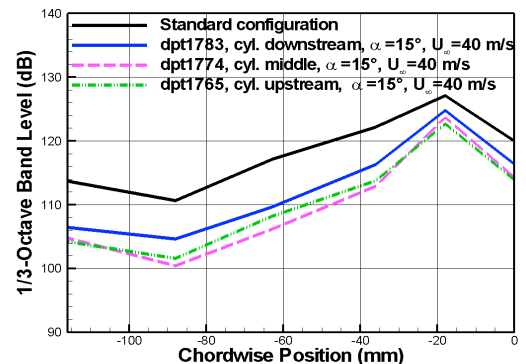


Figure 23: Effect of distance between gear and flap leading edge on surface pressure data, $U_\infty = 40\text{m/s}$, $\alpha = 7^\circ$, $f_m=1000\text{ Hz}$.



4. Effect of Wheels

To justify the omission of the wheels in the design of the generic gear model (see Section II-A), it was checked whether the wheels are indeed not important for interaction noise. This was done by mounting the two-wheel bogie of a 1:10 scaled center landing gear to the gear simulator (Figure 7). In order to prevent 'extraneous' noise from the wheels themselves, the wheel caps were covered with tape. The resulting interaction noise spectrum is compared to the standard spectrum in Figure 24. It turns out that the interaction noise levels are practically the same, apart from a slight increase for 4 kHz and higher. The evaluation of acoustic source plots shows that this increase is probably due to an increase in noise from the gear itself. This view is supported by the unsteady surface pressure results (not shown), which indicated no change due to the wheels. Therefore, the effect of the wheels on interaction noise seems to be small indeed.

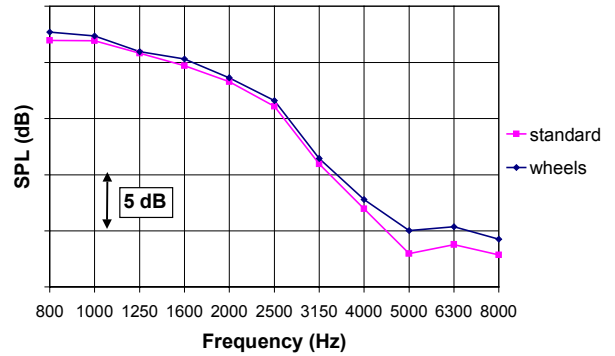


Figure 24: Effect of wheels on interaction noise ($U_\infty = 40 \text{ m/s}$, $\alpha = 7^\circ$).

5. Reduction Devices

A number of potential reduction devices was tested. One reduction device consisted of brushes at the upper or lower trailing edges of the main wing element, while another consisted of a porous material (thickness 4 mm) attached on top of the flap leading edge. The effect of these devices is shown in Figure 25. It turns out that the lower brush has practically no effect, but that the upper trailing edge brush leads to a noise reduction in the order of 1-2 dB. This reduction may be due to a reduction of (1) flap leading edge noise, and/or (2) main wing element trailing edge noise. In the first case the upper brush would modify the wake impinging on the flap, in the second case it would reduce trailing edge noise radiation from the main element directly. To distinguish between these two possibilities, we can look at the surface pressure results for the brushes (Figure 26). For the flap leading edge position a pressure level increase is observed for the lower trailing edge brush, while the upper trailing edge brush leads to a very small surface pressure level decrease (insert in Figure 26). Surface pressure levels on the flap's pressure side exhibit a level decrease for both the upper and lower trailing edge brushes. At higher frequencies (not shown), the upper brush resulted in larger surface pressure reductions at the flap leading edge (about 1 dB at 3.15 kHz). This finding may explain the noise reduction for the upper brush in Figure 25. This would imply that the upper brush reduces interaction noise by modifying the wake impinging on the flap, meaning that interaction noise is indeed radiated from the flap leading edge.

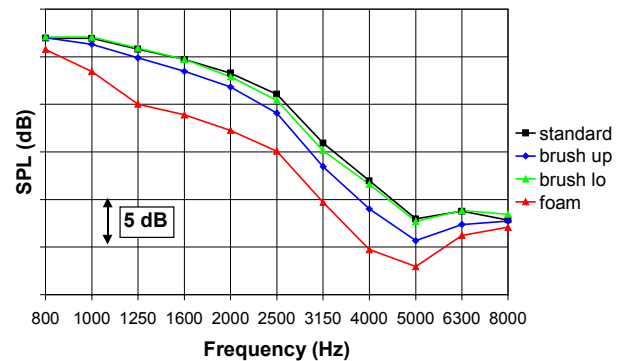


Figure 25 : Effect of reduction devices on interaction noise ($U_\infty = 40 \text{ m/s}$, $\alpha = 7^\circ$).

The foam around the flap leading edge shows a significant reduction of interaction noise of up to 5 dB (Figure 25). This supports the view that the interaction noise is in fact radiated from the flap leading edge rather than the trailing edge of the main wing element. With the foam attached to the flap leading edge most of the pressure sensors were covered, so that no surface pressure data are available for this configuration.

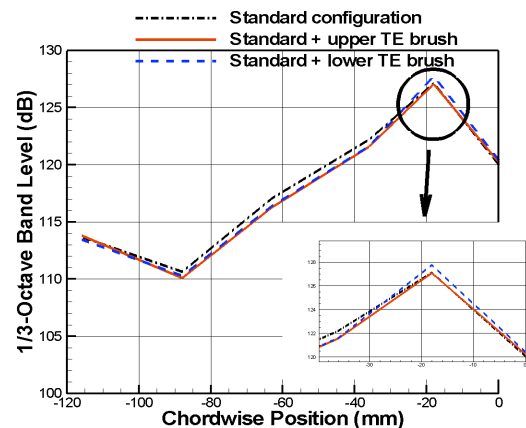


Figure 26: Effect of main wing trailing edge brushes on surface pressures, $U_\infty = 40 \text{ m/s}$, $\alpha = 7^\circ$, $f_m = 1000 \text{ Hz}$.



The beneficial effect of the devices on interaction noise was also observed in the farfield, confirming that a porous flap leading edge treatment is a promising reduction concept. In [Figure 27](#) the polar farfield noise directivities, with and without the upper trailing edge brush or the foam treatment at the flap leading edge, are shown for 1.0 and 1.6 kHz, representing the highest 1/3-octave band interaction noise levels. The farfield noise reductions are slightly smaller than the array-determined reductions in [Figure 25](#). This is probably due to the fact that the array focuses on the interaction noise, while the farfield levels also include noise from the gear itself.

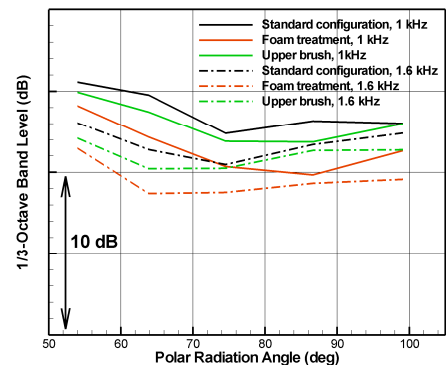


Figure 27: Effect of noise reduction devices
($U_\infty=40$ m/s, $\alpha=7^\circ$).

IV. Conclusions

An experimental study was performed into gear wake/flap interaction noise. Several measurement techniques were applied to determine the acoustic and aerodynamic characteristics of the flow. The test results clearly indicate the presence of interaction noise radiated from the flap leading edge downstream of the landing gear. It turns out that the interaction noise is most pronounced at low frequencies, where it dominates the noise from the landing gear itself. The gear rather than the cavity is found to be the most important contributor to the turbulent wake impinging on the flap. Flap unsteady surface pressure results indicate that this is due to the fact that the *gear* wake impinges on the *lower* flap surface, whereas the *cavity* wake is convected over the *upper* surface of the flap. The interaction noise shows no pronounced radiation directivity or dependence on angle of attack - except for a low frequency forward arc radiation. The noise levels are found to scale with U^6 versus Strouhal number. Increasing the distance between gear and flap results in a reduction of interaction noise in the order of a few dB. Even larger noise reductions can be obtained with a porous flap leading edge.

Acknowledgments

The authors would like to thank Wim de Wolf, Joop Gooden, and Frank Ganzevles for conducting and analyzing the wake measurements on the gear simulator. The contribution of Werner Dobrzynski to the performance and analysis of the interaction noise measurements is highly appreciated.

References

- ¹ Crighton, D.G., "Airframe Noise", in "Aeroacoustics of Flight Vehicles: Theory and Practice", NASA Reference Publication 1258, Vol.1, 1991.
- ² Barlow, J.B., Rae W.H., Pope A. "Low Speed Wind Tunnel Testing" John Wiley & Sons, Inc. 3rd edition, 1999.
- ³ Sijtsma, P., and Holthuisen, H., "Source Location by Phased Array Measurements in Closed Wind Tunnel Test Sections", AIAA paper 1999-1814, 1999.
- ⁴ Johnson, D.H., and Dudgeon, D.E., "Array Signal Processing", Prentice Hall, 1993.
- ⁵ Amiet, R.K., "Refraction of Sound by a Shear Layer", Journal of Sound and Vibration, Vol. 58, No. 2, pp 467-482, 1978.
- ⁶ Brooks, T.F., and Humphreys, W.M., "Effect of Directional Array Size on the Measurement of Airframe Noise Components", AIAA paper 99-1958, 1999.
- ⁷ Oerlemans, S., and Sijtsma, P., "Acoustic Array Measurements of a 1:10.6 Scaled Airbus A340 Model", AIAA paper 2004-2924, 2004.
- ⁸ Hutcheson, F.V., and Brooks, T.F., "Effects of Angle of Attack and Velocity on Trailing Edge Noise", AIAA paper 2004-1031, 2004.
- ⁹ Home, W.C.; Hayes, J.A.; Ross, J.C.; Storms, B.C.: "Measurements of Unsteady Pressure Fluctuations on the Surface of an Unswept, Multi-Element Airfoil", AIAA/CEAS Aeroacoustics Conference, Paper-No. 97-1645, Atlanta/GA, May 12-14, 1997.
- ¹⁰ Guo, Y.P.; Joshi, M.C.; Bent, P.H., Yamamoto, K.J.: "Surface pressure fluctuations on aircraft flaps and their correlation with far-field noise", Journal of Fluid Mechanics, Vol. 415, pp. 175-202, Cambridge University Press, 2000.
- ¹¹ Blake, W.K., "Mechanics of Flow-Induced Sound and Vibration", Academic Press, 1986.
- ¹² Oerlemans, S., and Migliore, P., "Aeroacoustic Wind Tunnel Tests of Wind Turbine Airfoils", AIAA paper 2004-3042, 2004.